Potential of spent fluid cracking catalyst (FCC) waste for low-carbon cement production. Effect of treatments to enhance reactivity

Z. Lei, S. Pavia [*]

Department of Civil Engineering, University of Dublin Trinity College, Ireland

ARTICLE INFO

ABSTRACT

Spent fluid cracking catalyst (FCC) waste is produced to convert petroleum crude oil into gasoline, and its main component is a reactive zeolite known as faujasite. This paper studies low-energy treatments to enhance reactivity. When untreated, the spent FCC has outstanding activity, and a fast set which delivered significant strength (6–10 MPa) and a high mechanical index (MI=14). Calcination (up to 800 °C) is not enough to amorphize the faujasite and increase reactivity. However, NaOH-fusion is highly efficient. Even at low temperature (450 °C), NaOH-fusion breaks down the zeolite structure, dissolving Si^{4+} that forms cementing hydrates with high Ca/Si and Si/Al ratios which delivered high strengths. NaOH-fusion at 450 °C totally amorphized the zeolite resulting in high strength (9–13 MPa) and outstanding MI>22; superior to pozzolans, and closer to cementitious materials. Fusion at 600 °C reorganises some of the amorphous phase into a silicate whose hydrates provided the greatest strengths (over 16 MPa) and an outstanding MI of 24.

Na_2CO_3-fusion at 600 °C did not alter the spent FCC but provided CO_3^{2-} which formed calcite cements. These initially densified the matrix providing strength but lowered long-term strength and workability.

Acid-etching partially dissolved spent FCC particles which improved early activity but caused a loss of soluble Si^{4+} and Al^{3+} that reduced the ultimate strength. Due to the low organic matter in the spent FCC, oxidation did not increase reactivity.

The spent FCC is highly pozzolanic, it can safely reduce the embodied carbon of cements: concentrations of heavy metals are either traces or insignificant. Therefore, they can easily immobilise in a stable matrix.

1. Introduction

The fluid catalytic cracking process is used in the petrochemical sector to convert petroleum crude oils into gasoline and other products [1]. The process uses zeolite-based catalysts which deactivate over the course of the cracking process losing their catalytic capacity, hence becoming a waste [2]. The modern refinery FCC units operate 24 hours a day, and circulate about 55,900 t of catalyst per day [3]. The annual global use of catalysts in cracking processes has been estimated at 800, 000 tons, with refineries being the principal consumer [1,4]. The use of refinery catalysts will increase by approximately 5% in the next decade [5].

FCC deactivates reversibly, as a consequence of side reactions that eventually give coke, and irreversibly: either as a result of sulphur, vanadium and nickel contamination in the crude feedstock or due to the dealumination of the zeolite catalyst [6,7]. In either case, the spent catalyst is typically discharged every three to four weeks.

The term spent FCC includes several compounds that are sometimes classified as ignitable and toxic (hazardous) waste. Some regulations consider spent FCCs as a whole, and they classify them as ignitable and toxic. However, this generalisation is controversial and, as demonstrated by several scientists, many spent FCCs are neither toxic nor ignitable. Fu et al [8] studied 21 spent FCCs, and concluded they were neither flammable nor corrosive or reactive. Their leaching toxicity and toxic substance study found that, except for one sample, the waste catalysts did not have any leaching toxicity or toxic substance content.

The composition of spent FCCs depends on the nature of the catalyst and the additives, the fluid cracking process, and the varying proportions of fresh catalyst and regenerated catalyst. Furthermore, the characteristics of the feedstock added to different units vary, and this results in large differences in the concentration of pollutants [8]. Wang et al. [9] investigated the toxicity of 17 types of spent FCCs on aquatic life, and concluded that their toxicity depends on the concentration of Ni, La, Mn, Co and Ca. The chemical and mineral composition of the

present spent catalyst indicate that it is safe for inclusion in a durable matrix as discussed below.

Many spent FCCs are classified as non-hazardous wastes and hence landfilled (Ferella et al. 2016; [10]). The USA does not consider spent FCCs as hazardous waste, and they do not manage them as hazardous wastes [11]. However, other catalysts such as spent hydroprocessing catalysts, are classified as hazardous wates (due to their self-heating behaviour and toxic chemical content), and managed consequently [12]. In Europe, spent FCCs are classified as "general solid waste" (number 160,804), and only some (with toxic content) are managed as hazardous wastes [13]. China included spent FCCs in their "National Hazardous Waste List" in 2016 [14]. However, this caused a major dispute because the risk posed by spent FCC is controversial. Fu et al. (201) report that spent FCC is not a hazardous waste. They carried out a leaching toxicity and toxic substance study of 21 spent FCCs and found that, except for one sample, the waste catalysts had neither leaching toxicity nor toxic substance content.

According to the safety data of the producers, the present spent FCC ignites over 400 °C; the temperature of ignition of the zeolite which is the main component (1907/2006/CE). According to these data, the spent catalyst can be dangerous if swallowed or inhaled in significant amounts. However, this paper intends to immobilise it in a solid, durable matrix. We investigate the pozzolanic activity of the waste catalyst so that it can be immobilised in a stable matrix; either as partial Portland cement (PC) clinker replacement or as a precursor to produce alkali activated materials. Previous authors found that recycling spent FCC in PC is an effective means of stabilisation of vanadium and nickel at levels of 3518 and 3225 ppm respectively [15]. These levels are much greater than the V and Ni levels in this paper.

Construction materials are responsible for high greenhouse gas (GHG) emissions which exacerbate global warming and climate change; in particular PC which is the most used binder in construction. The total GHG emissions of a material (resulting from production, construction, maintenance, repair, demolition and disposal) are known as embodied carbon (EC). To reduce the EC of construction, waste is repurposed as PC clinker replacement. Metallurgical slags and fly ash wastes have been used in such manner for decades. These and other wastes containing silica and/or alumina can be activated with lime or alkali metals to produce cements with lower EC than traditional PCs. Duxson et al. [16] found that alkali-activated FA and metakaolin cements save 80% of CO_2 emissions when compared to equivalent PC products. According to Alelweet and Pavia [[17] a], a suitably activated, high-calcium slag waste attained strength like equivalent CEM II mixes at half the embodied energy and carbon emissions.

The main constituent of the spent FCC is a crystalline, synthetic, Y-type zeolite: a faujasite with a Si/Al ratio = 1.5–3 which increases during the cracking process [18]. A typical modern cat cracking catalyst has four major components: Zeolite Matrix Filler Binder [19]. According to the author, the matrix consists of alumina which can be active during the catalytic process. The filler is a clay, usually kaolin [$Al_2(OH)_2$, Si_2O_5] which provides structural integrity and can also be active. The binder is the glue that holds the zeolite, matrix and filler together. It may or may not have catalytic activity.

Zeolites consist of SiO_4^{4-} and AlO_4^{4-} tetrahedra, joined forming open structures of large surface area, with crossing channels and cages which usually enclose water molecules and alkaline or alkali-earth cations [18]. Zeolite lattices have a network of very small pores, hence zeolites are sometimes called molecular sieves [19]. The cracking process changes the chemical composition and structure of the zeolite [19]: the zeolite is subjected to thermal and hydrothermal deactivation in the regenerator, and exposed to feedstock contaminants such as vanadium and sodium in the reactor.

It is well known that zeolites have significant pozzolanic activity, reacting with lime to form cementing hydrates. Therefore, they have been used as pozzolans for thousands of years, since Roman times, probably earlier. Liguori et al. [20] summarise the reactions that occur in a zeolite-lime system as follows: dissolution of solids (lime and zeolite); ion exchange between the cations in the zeolite and the Ca^{2+} released by the lime; zeolite breakdown and conversion into a transient amorphous material; and precipitation of hydrates (calcium aluminate hydrates- C-A-H - and calcium silicate hydrates - C-S-H). Today, natural zeolites are used in cement production: as 6–35% PC clinker replacement to create CEM II A/B P/Q products (EN 197–1).

The pozzolanic activity of the synthetic zeolite comprising the spent FCC has been proven by previous authors [21,22]. Payá et al. [23] conclude that it has pozzolanic activity like metakaolin (MK). Several authors studied PC (mainly CEM I) blended with spent FCC. Su et al. [24] and Payá et al. [25] state that the spent catalyst can replace up to 15–20% of PC without compromising the material quality. Payá et al. [25] found that the strengths of PCs blended with spent FCC were similar or slightly greater than the control mortar made with 100% PC. Some authors found that the properties of the blended cements were superior than those of the control material [10,26]. However, others found the opposite [27]. In these studies, the spent FCC was untreated, and the pozzolanic cements were not investigated. This paper intends to fill this gap by treating a spent FCC to enhance its reactivity and study the resultant cements.

Calcination treatments are widely recognized as an effective method for improving reactivity. Research on this subject has been ongoing for decades, dating back to the 1950s [28]. Calcination has proven successful for materials such as clays [29,30], coal waste [31,32], paper sludge [33], and sugar cane straw waste [34]. Heat alters clay mineral structures: low temperatures cause dihydroxylation, releasing Al and Si that became available for reactions (Bergaya & Lagaly, [35]). Hydrous aluminium oxides with layered atomic structures such as gibbsite and boehmite in bauxites also activate with heat [17]. Calcination is an important treatment for wastes with cementing potential because, not only it can enhance their reactivity, but it can also remove the organic matter (carbon) which lowers workability and raises water demand to dangerous levels that can cause shrinkage cracks and undermine strength [36–38]. Furthermore, calcination can turn amorphous or semi-amorphous content into crystalline phases of lower reactivity, and this moderates the reactivity of excessively reactive wastes that produce flash set being unworkable [17,37]. Lei and Pavia [37] investigated the reactivity of alum sludge waste (AS). The AS calcined at 600 °C was excessively reactive, and useless as a cementing material due to the occurrence of an exothermic reaction and flash set during mixing. However, calcination at 800 °C converts some amorphous content into more orderly γ-Al2O3 which avoids flash set and allows for proper handling.

Furthermore, calcination treatments cause less environmental impact than calcination and grinding for PC production. Calcination of bauxite and other aluminous reactive wastes at relatively low temperature can procure great strengths at low environmental impact [39]. The authors measured the pozzolanic and hydraulic properties of raw and thermally activated bauxite for binder production. They conclude that sintering bauxite at 800 °C slightly raised the embodied carbon and embodied energy of the resultant material but nearly doubled the strength when compared to equivalent CEM II products of higher embodied carbon and embodied energy (37 vs 60 MPa).

Chemical treatments such as acid etching and oxidation can also enhance pozzolanic activity. Ismail et al. [40] found that, after acid treatment, the surface of palm oil clinker became porous and pozzolanic activity increased. However, de Lima & Cordeiro [41] reported that acid etching can remove alkalis and alkali metals (Ca, Mg) which lowers reactivity. Oxidation can remove organic compounds which retard cement hydration [42]. Alkali fusion is widely reported as an effective method to synthesise zeolite and to recover metals from waste [43–45]. Alkali fusion involves mixing the waste with an alkali at high temperature. Alkali refers to a base such as a carbonate or hydroxide of an alkali metal. Often, sodium hydroxide or sodium carbonate are used [46,47]. Recently, this technique has been used to convert low-reactivity

crystalline wastes into pozzolans. Mao et al. [48] report that the fusion of basalt with NaOH increased reactivity by approximately 30%. Liu et al. [49] found that crystalline minerals in mine tailings turned into amorphous sodium aluminosilicate after alkali fusion thereby increasing the reactivity.

Research on pozzolan activation has developed in recent years, but the activation of spent FCC, an industrial waste with a large yield, has received insufficient attention. This research intends to optimise the activity of the spent FCC by increasing particle reactions, using adequate activation procedures which are proposed based on the characteristics of the spent FCC. We measure the reactivity of spent FCC, after calcination, oxidation, acid etching and alkaline fusion, with chemical and physical methods. Tests are conducted with lime rather than PC to enable a simpler chemical system where reactions are well known and can be better followed, and research variables are more controlled. However, the results apply to both lime and PC systems because both pozzolanic and supplementary cementitious materials (SCMs) react with lime, either added in the paste or released on PC clinker hydration.

2. Materials and methods

2.1. Characterisation of the spent FCC

The particle size distribution was determined by laser diffraction with a laser particle size metre (Mastersizer 3000, Malvern Instruments), using water as the dispersing agent.

The chemical composition of the FCC was determined with X-ray fluorescence (XRF) analysis and inductively coupled plasma optical emission spectrometry (ICP-OES). The results are expressed as a percentage by oxides and elemental concentration respectively. The calculation method of the XRF results (ME-ICP06) is not normalised. Therefore, the results are not brought up to 100% by applying factors but, rather, the method reports the results as measured, with $\pm 2\%$ tolerance for each analyte. As a result, our oxide total slightly exceeds 100%. The mineral composition of the spent FCC and FCC/lime pastes (cured for 28 days) were analysed with X-Ray Diffraction (XRD) using the powder method, with a Burker D5000 apparatus, scanning between $2°$ and $70°$ 2θ. The powder diffraction data were interpreted with EVA software and a PDF-4+ 2022 database. The crystallinity/ amorphousness of the spent FCC was estimated as the differential of the percentage area of the crystalline region to the total area of the diffractogram. The loss on ignition (LOI) was measured as weight loss by calcination at $1000°C$ for 1 h. The accuracy of the measurement is 0.1 mg. According to the producers, the differences between batches of spent catalysts (in terms of the percentage of metal adsorbed and active surface) are minimal, and the matrix-zeolite structure is essentially constant.

2.2. Treatment of the spent FCC

All the treatments have low-energy input to be consistent with low carbon production.

Calcination: The raw spent FCC was calcined in an electrical furnace at temperatures of 300–800 °C for 2 h and cooled naturally.

Oxidation: The spent FCC was oxidized with a 15% hydrogen peroxide -H_2O_2- solution. The FCC-H_2O_2 mixtures were aged at room temperature for 24 h, and then dried in an oven at 105 °C. The reaction was slightly exothermic and caused remarkable oxygen evolution producing abundant bubbles.

Acid etching: The spent FCC was etched with a 0.1 M HCl solution. The FCC / 0.1 M HCl mix was aged at room temperature for 24 h, and then filtered and washed with distilled water. The residues were dried in an oven at 105 °C. The reaction did not produce any heat or effervescence.

Alkali fusion: The spent FCC was mixed with 15%NaOH and calcined at 450/600 °C for two hours. A further mix was produced with FCC and 20%Na_2CO_3 of $\geq99.8\%$ purity and calcined at 600 °C for two hours.

Table 1

Mix design for the strength test. The setting time, XRD and SEM specimens are the same mixes without sand. ** Water / binder. The binder consists of spent FCC and CL90s.

Notation	Treatment	Composition				
		FCC	CL90s	Sand	Water	w/b**
FCC/raw	None	1	1	3	1.5	0.75
FCC/300	Calcination at 300 °C for 2h	1	1	3	1.5	0.75
FCC/400	Calcination at 400 °C for 2h	1	1	3	1.5	0.75
FCC/500	Calcination at 500 °C for 2h	1	1	3	1.5	0.75
FCC/600	Calcination at 600 °C for 2h	1	1	3	1.5	0.75
FCC/700	Calcination at 700 °C for 2h	1	1	3	1.5	0.75
FCC/800	Calcination at 800 °C for 2h	1	1	3	1.5	0.75
FCC/H_2O_2	Oxidation with 15% H_2O_2 for 24h	1	1	3	1.5	0.75
FCC/HCl	Etching with 0.1 N HCl for 24h	1	1	3	1.5	0.75
FCC/NC	Fusion with 20% Na_2CO_3 at 600 °C for 2h	1	1	3	1.8	0.90
FCC/NH/450	Fusion with 15%NaOH at 450 °C for 2h	1	1	3	1.5	0.75
FCC/NH/600	Fusion with 15%NaOH at 600 °C for 2h	1	1	3	1.5	0.75
Lime/0.75	–	0	2	3	1.5	0.75
Lime/0.90	–	0	2	3	1.8	0.90

The solution-to-solid ratio for both acid etching and oxidation is 10:1. Alkali-fusion has no solution, and the alkali content is 25%.

2.3. Mix design

The mixing proportions of FCC, hydrated lime (CL90s) and sand are constant at 1:1:3. A siliceous sand of grading and composition like the standard CEN sand, and a hydrated lime of European designation CL90s were used. The water content was adjusted until the sample provided a desirable workability, measured as an initial flow diameter of 165 mm [50]. In addition, two reference specimens were prepared with CL90s and sand at w/b = 0.75 and 0.90, respectively. The mix proportions appear in Table 1. All solid components (FCC, CL90s, sand) were mixed for 2 min in a mechanical mixer. Water was then added and mixed for a further 5 min. The fresh slurry was cast into 160 × 40 × 40 mm steel moulds and cured, wrapped in polyethene film to prevent moisture loss. The specimens were demoulded after 24 h and stored in a curing room at 20 ± 3 °C, under damp hessian.
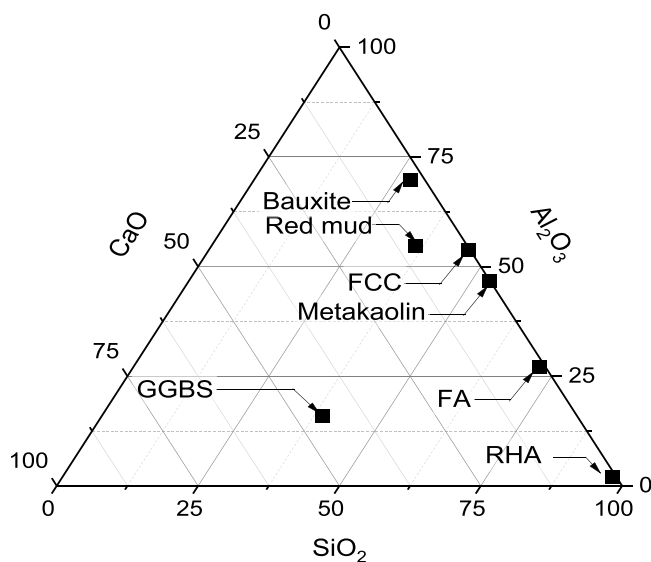
2.4. Reactivity by the Chapelle test

The pozzolanic activity of both the raw and treated spent FCC was measured according to the Chapelle test. This is a standard test that measures the amount of portlandite (Ca(OH)$_2$) that the FCC is capable of binding in an aqueous solution as a measurement of the pozzolanic activity. 1 g of FCC was mixed with 2 g of CaO and 250 ml of distilled, CO_2 free water. The suspension was shaken for 16 h at 90 °C in a water bath. The free Ca^{2+} (dissolved with a saccharose solution) was determined by means of HCl titration. The amount of pozzolanic material was calculated using Eq. (1).

$$mg\ CaO\ bound\ per\ gram\ of\ material = \frac{112(v_3 m_3 - v_2)F_c}{m_4 m_3 m_2} \qquad (Eq.1)$$

Where: m_2 = grams of pozzolanic material
m_3 = grams of CaO mixed with pozzolanic material
m_4 = grams of CaO in the blank test

Table 2

Chemical composition and grading of the FCC.

Chemical composition (XRF)	wt%	Heavy metal content (ICP-OES)	ppm	Notes
SiO₂	41.7	V	634	
Al₂O₃	49.0	Ni	336	
Fe₂O₃	1.28	Co	30	
CaO	0.19	Cu	20	~trace
MgO	0.07	As	20	~trace
Na₂O	0.29	Zn	26	
K₂O	0.16	Cd	<0.5	trace
Cr₂O₃	0.04	Hg	1	trace
TiO₂	1.00	Tl	<10	trace
MnO	0.01	Pb	18	~trace
P₂O₅	0.26	Particle size distribution/specific surface area (laser diffraction)		
La₂O₃	2.50			
SrO	<0.01	D [3,2] particle size	66.9 μm	
BaO	0.02	D [4,3] particle size	78.1 μm	
LOI at 1000 °C	3.70	D₅₀ particle size	72.3 μm	
		Specific surface area	85.44 m²/kg	

The table above uses subscripts; rendered in LaTeX: SiO_2 41.7, Al_2O_3 49.0, Fe_2O_3 1.28, CaO 0.19, MgO 0.07, Na_2O 0.29, K_2O 0.16, Cr_2O_3 0.04, TiO_2 1.00, MnO 0.01, P_2O_5 0.26, La_2O_3 2.50, SrO <0.01, BaO 0.02, LOI at 1000 °C 3.70. Heavy metals: V 634, Ni 336, Co 30, Cu 20, As 20, Zn 26, Cd <0.5, Hg 1, Tl <10, Pb 18. D_{50} particle size 72.3 μm.

Fig. 1. Chemical composition of the spent FCC waste, compared with some pozzolans and supplementary cementitious materials in Walker & Pavía [52]; Alelweet & Pavia (2022).

$v_2 = $ milliliters of $0.1M$ HCl consumed by the sample solution

$v_3 = $ millilitres of $0.1M$ HCl consumed by the blank test

$F_c = $ correction factor of $0.1M$ HCl standard solution

2.5. Reactivity by strength development and mechanical activity index

The strength development of spent FCC-lime mixes was monitored over 28 days. The unconfined compressive and flexural strengths were measured with a Zwick loading machine in accordance with EN 459–2. Also, the mechanical activity index (MI) was calculated according to EN 450–1. The MI displays reactivity as the ratio of the compressive strength of a FCC-lime mix to a standard lime mix. Prismatic specimens of $160 \times 40 \times 40$ mm were tested. The results are the arithmetic mean of 3/6 specimens.

2.6. Setting times

The initial and final setting times of the spent FCC pastes were measured in accordance with EN 196–3 using the Vicat apparatus. The setting times helped estimate the reactivity of the spent FCC and the cementing/setting ability of the early hydrates.

2.7. Scanning electron microscopy and energy dispersive X-ray spectroscopy (SEM-EDX)

SEM-EDX analyses were conducted to investigate the surface characteristics of the spent FFC catalyst particles before and after the treatments. The SEM apparatus was also used to study the cements in the FCC-lime pastes (raw and treated) at 270 days. The EDX technique was used for the elemental analysis of the cements formed. The equipment consists of a Zeiss ULTRA plus apparatus with a 20 mm² Oxford Inca EDX detector. Images and composition spectrums were taken for powder and paste specimens coated with gold/palladium to avoid electric charging.

3. Results and discussion

3.1. Characterization of the raw spent FCC

The chemical composition and grading of the spent FCC appear in Table 2. It is mainly composed of SiO_2 and Al_2O_3. When compared with other pozzolans and supplementary cementitious materials (Fig. 1), the spent FCC displays high Al, moderate Si content, and traces of Ca. The spent catalyst composition is like metakaolin, both consisting of over 90% SiO_2 and Al_2O_3. The composition exceeds the current chemical requirements for the use of pozzolans and cementitious materials in building standards (Table 3), hence the spent catalyst can produce a highly active pozzolan. Also, the Mg and P_2O_5 contents are extremely low, consequently meeting standard requirements (Table 3). The main components (silica and alumina) account for over 90% of the total, agreeing with other spent catalysts in the literature [3,8,51].

In relation to the hazardous characteristics of spent FCCs, the focus is on their heavy metal content because, when directly landfilled, the leaching of heavy metals such as nickel, zinc, barium and arsenic can pose risks to the quality of the groundwater [51]. Heavy metals have numerous industrial applications; hence they are widely found in our environment which has raised concerns over their toxicity. Contamination by heavy metals can occur through metal corrosion, atmospheric deposition, soil erosion and leaching, metal processing, coal-burning power plants, petroleum combustion, nuclear power stations, high-tension lines, plastics, textiles, microelectronics, wood preservation and paper processing plants [55]. Some of the metallic elements in spent FCC waste such as cobalt, copper, chromium, iron, magnesium, manganese and zinc, are essential nutrients required for physiological functions. However, arsenic, cadmium, lead and mercury are considered

Table 3

Compliance of spent FCC with standard requirements for the use of FA, GGBS and natural pozzolans in concretes and other materials. All results in % by mass.

	$\sum SiO_2, Al_2O_3, Fe_2O_3$	SO_3	MgO	Cl⁻	LOI	Total P_2O_5
EN 450 - FA requirements	≥ 70	≤ 3	≤ 4	≤0.10	< 5	<5.5
ASTMC618-pozz.requirements	50–70	4–5	–	–	<10	–
EN 15,167-GGBS requirements	–	<2.5	≤ 18	≤ 0.10	≤ 3	–
FCC	92	–	0.07	–	3.7	0.2
FA [53]	89	1.4	1.0	0.04	4.9	0.5
GGBS [54]	49–44	2.2	8	0.03	<1	0.4

Table 4
LOI of the spent FCC.

Temperature	% weight loss	Equivalence
0 to 105 °C	1.35	Water
105 to 550 °C	0.00	Organic material and water loss from clay minerals
550 to 950 °C	0.77	Release of H_2O/CO_2
Residue remaining after 950 °C	97.88	Oxide/silicate residue

toxic [55]. In the present spent FCC, there are only traces (<10 ppm) of cadmium, mercury, thallium and lead, and arsenic is close to the tracing concentration (Table 2). Only nickel and vanadium are present in greater amounts, however insignificant. Sun et al. [15] successfully stabilised vanadium and nickel, in a PC matrix, at levels of 3518 and 3225 ppm respectively, which are much greater than the levels in this paper (V = 634 ppm and Ni = 336 ppm).

Heavy metals such as Ni and V enter the FCC from the petroleum feedstock during the cracking process. The toxicity of vanadium is considered low, and only certain compounds can become toxic. Evidence suggests that vanadium and its compounds are not carcinogenic, and vanadium is not classified as carcinogenic by the Environmental Protection Agency [56]. Nickel is found naturally, and it is essential to plants. It is used widely in industry in alloys, stainless steel and batteries (electric vehicles). Nickel is not cumulative, but it is processed by the kidneys and removed from the body; average daily exposure does not pose a threat to human health, but oral consumption or chronic inhalation may be toxic [57].

The content of lanthanum, a rare earth element, is significant. In terms of toxicity, lanthanum has not known harmful effects on humans, and it is difficult to absorb even if ingested [58]. It has numerous industrial applications such as electric car batteries and catalysts [58]. When injected into the brain, it acts as a painkiller, similarly to morphine and other opiates [58–60].

As indicated by the loss on ignition (LOI) test (Table 4), the spent catalyst has low organic matter content. This is due to the temperature of the cracking process. The cracking reaction is endothermic. It occurs between 500 and 760 °C, and the heat required for cracking is produced by burning a small portion of the feedstock [61]. Hot catalyst is combined with pre-heated feedstock, and the temperature at the bottom of the riser is typically c. 550 °C. Depending on the conditions (such as oxygen availability), the temperature can reach up to 760 °C, and a typical FCC catalyst has an average lifetime of about 1 month [61].

The particle size distribution of the spent catalyst appears in Fig. 2. The results show that it is coarser and more monogranular (lower spread of particle sizes) than other pozzolans and supplementary cementitious materials such as FA and GGBS. The close D [3,2] and D [4,3] values indicate that the catalyst particles are regular and rounded.

The SEM evidenced that the catalyst particles tend to spherical, and their size and shape are consistent (Fig. 3) agreeing with the laser diffraction results. Further magnification reveals rough, porous surfaces of significant specific surface area- SSA. The SSA of the catalyst particles is lower than other pozzolans and SCMs (Table 5). However, it is underestimated because the laser assumes that the particles are solid and
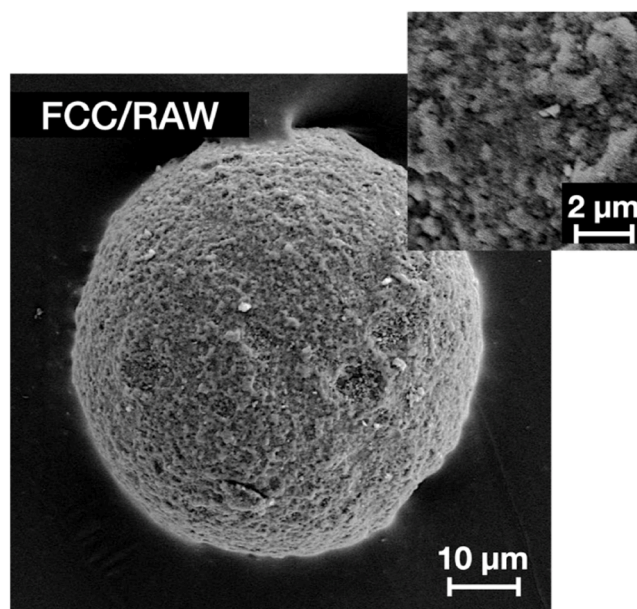

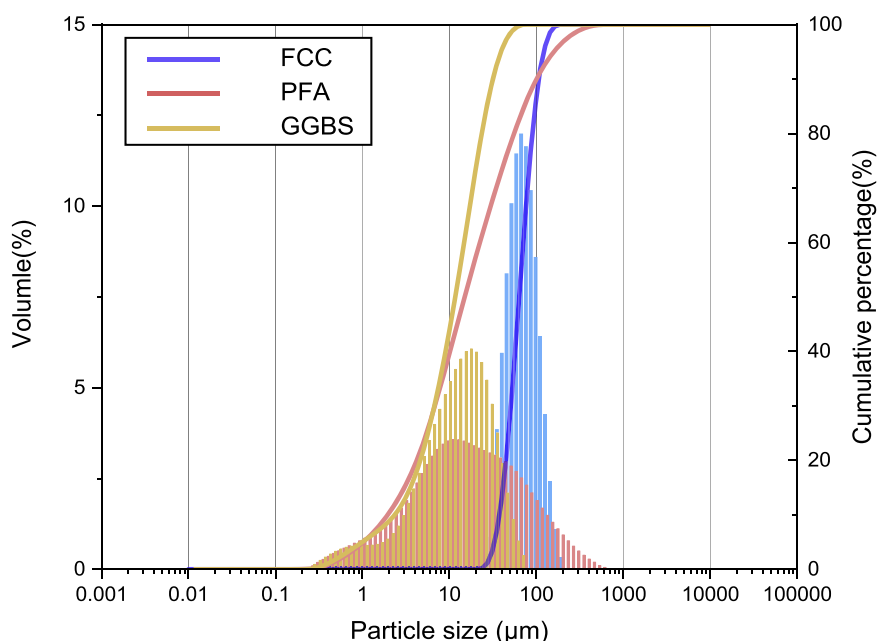**Fig. 3.** Shape and surface of the raw spent FCC particles.

Fig. 2. Particle size distribution of the spent FCC compared with FA and GGBS.

Table 5
SSA of the spent FCC particles compared with other pozzolans and SCMs in * Alelweet & Pavia 2022; ** [38].

Material	Specific surface area (SSA) m²/g
FCC	0.08 (laser value)
	0.17 (with conversion factor)
Bauxite*	17.92
Red Mud*	9.35
GGBS*	1.95
FA*	6.50
CEM II*	1.88
RHA**	13.70

spherical rather than very porous. Therefore, a correction factor of 2 is applied based on Gómez-Tena et al. [62] who, determined this factor, for rounded particles, based on experimental laser diffraction and BET (Brunauer, Emmett and Teller) measurements.

The main crystalline phase in the spent FCC is the zeolite faujasite (Figs. 4 and 5). As aforementioned, faujasite is a microporous aluminosilicate composed of $[SiO_4]^{4-}$ and $[AlO_4]^{5-}$ tetrahedra. It has high porosity and the ability to exchange intercluster ions, hence it is considered at least as reactive as vitreous pozzolans [63]. Two high-temperature aluminosilicate polymorphs, sillimanite and kyanite, were also identified (Fig. 5). These are residues from the catalytic cracking process as they are used as active fillers during the process [64, 65]. Traces of anatase (TiO_2) were also found. Anatase is added to trap vanadium in order to prevent its passivating effect [66].

3.1. Effect of the treatments on the spent FCC

Zeolites undergo structural changes when calcined including: (i) the removal of water and/or organic molecules; (ii) transformation into a
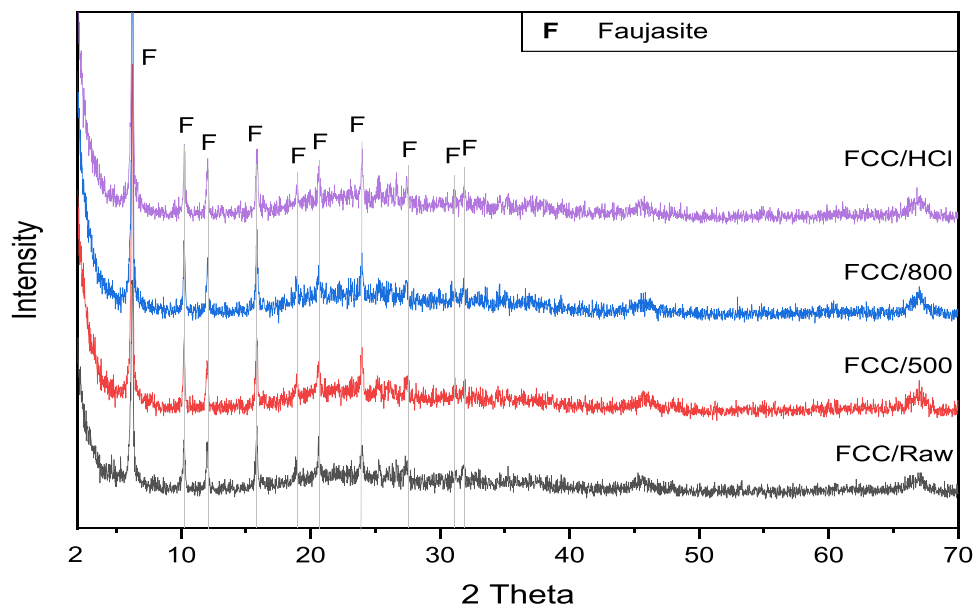
Fig. 4. Mineral assemblage (main phases) in the raw, calcined and etched spent FCC.
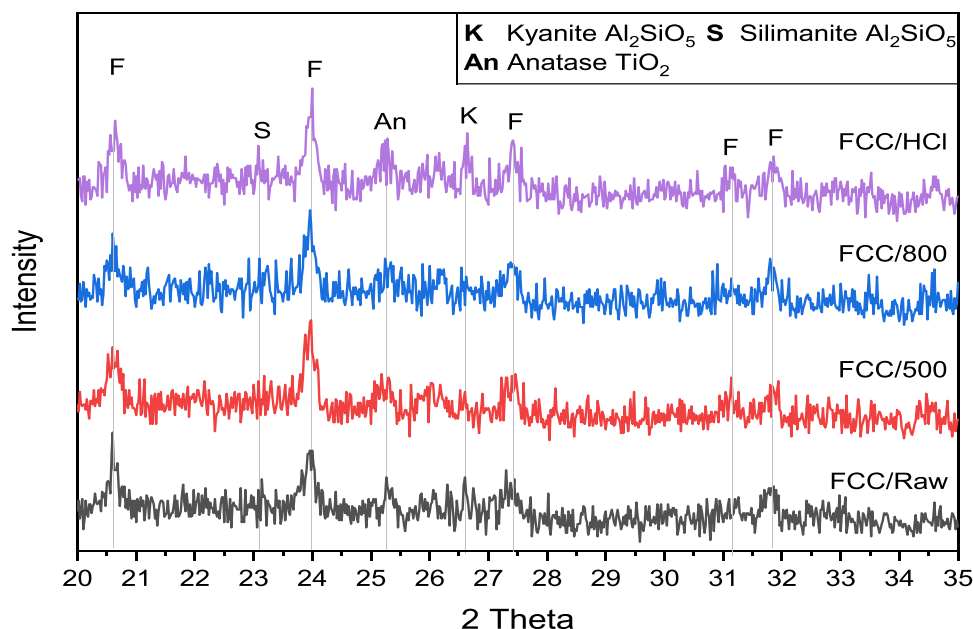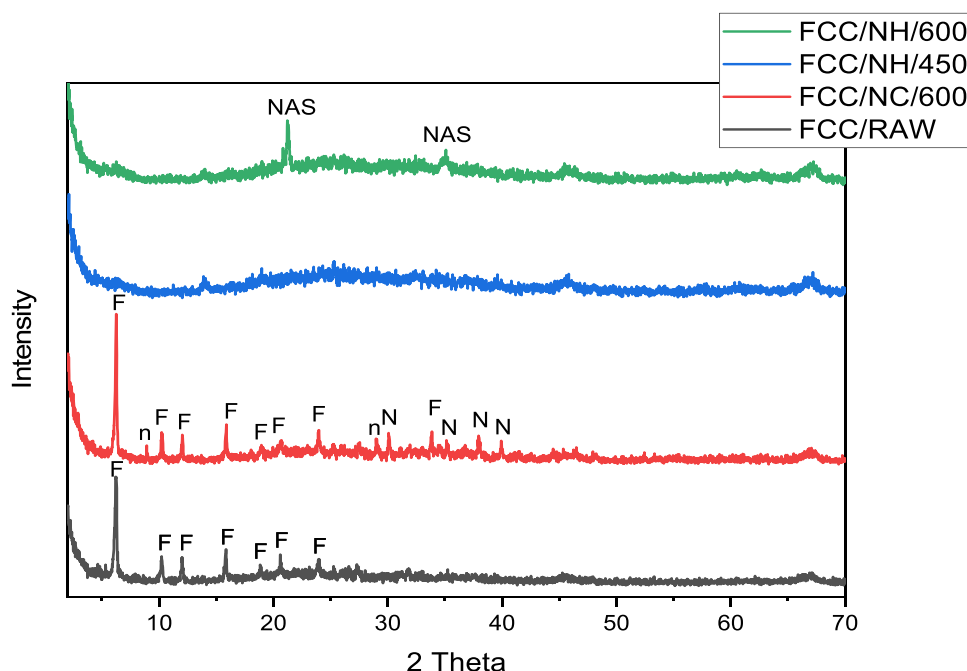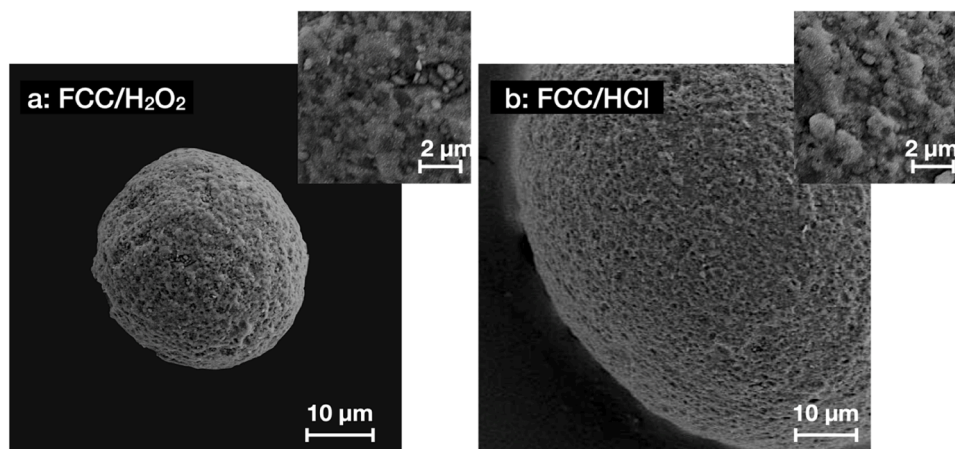

Fig. 5. Subsidiary mineral phases in the raw, calcined and etched spent FCC.

Fig. 6. Mineral assemblage of the alkali-fused spent FCC. NH- Na(OH). NC- Na_2CO_3. F: Faujasite - $H_{7.7}Al_{42.56}Si_{139}O_{345.6}$. N: Natrite -$Na_2CO_3$. n: Trona - $Na_3H(CO_3)_2$ $2H_2O$.
NAS: Sodium aluminium silicate - $Na_{1.15}Al_{1.15}Si_{0.85}O_4$.

Fig. 7. SEM micrographs of (a) oxidised, (b) HCl-etched spent FCC particles.

metastable phase; (iii) structural collapse and (iv) amorphization [6]. However, the XRD evidenced that no significant changes take place in the mineralogy of the spent FCC up to 800 °C (Figs. 4 and 5). This agrees with Li and Rees [67] who demonstrated that, despite its open structure, faujasite is extremely stable at high temperatures up to 900–1000 °C.

As it can be seen from Fig. 6, fusion with Na_2CO_3 at 600 °C (FCC/NC/ 600) produces sodium carbonates natrite (Na_2CO_3) and trona ($NaHCO_3$) which coexist with faujasite. This indicates that fusion between the zeolite and the carbonate did not take place during the treatment. This is due to the melting point of sodium carbonate (c.820 °C, [68]) being greater than the calcination temperature (600 °C). This agrees with Feng et al. [69] and Choi et al. [70] stating that calcination temperature needs to be far beyond the melting point of Na_2CO_3 for the carbonate to break and provide Na^+ and CO_3^{2-} to react with the pozzolan.

In contrast, fusion with NaOH, at both 450 and 600 °C, altered the mineral composition of the spent FCC (Fig. 6). At 450 °C, the spent catalyst has become totally amorphous, and the characteristic peaks of

the zeolite have disappeared. At 600 °C, part of the amorphous phase has transformed into crystalline sodium aluminium silicate ($Na_{1.15}Al_{1.15-}Si_{0.85}O_4$ - N-A-S). Therefore, alkali fusion at 600 °C released Na^{2+} and OH^- (the NaOH's melting point is c.320 °C), and these collapsed the faujasite crystals, part of which later reorganised to form N-A-S.

The SEM evidenced changes caused by the treatments. Oxidation increased surface roughness (Fig. 7a), probably due to the removal of coke generated during the cracking process agreeing with Vaičiukynienė et al. [42]. Acid etching smothered the rough catalyst particles (Fig. 7b). Shi and Day [71] report that acid treatment dissolves pozzolans and can form gels on the surface. However, the SEM showed no new-formed phases on the etched particles. This agrees with the XRD results showing no changes in the mineralogy of the acid-etched catalysts (Figs. 4 and 5). Calcination at 800 °C smothered the particle surface (Fig. 8), and macropores were no longer evident.
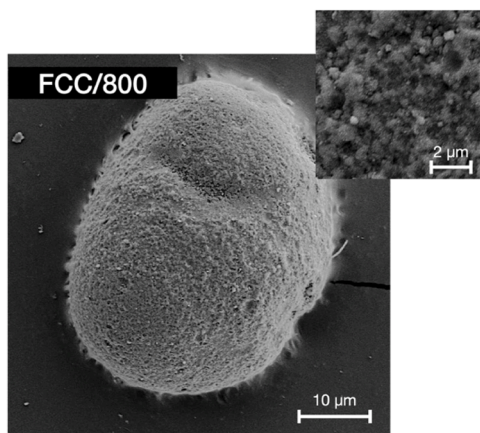
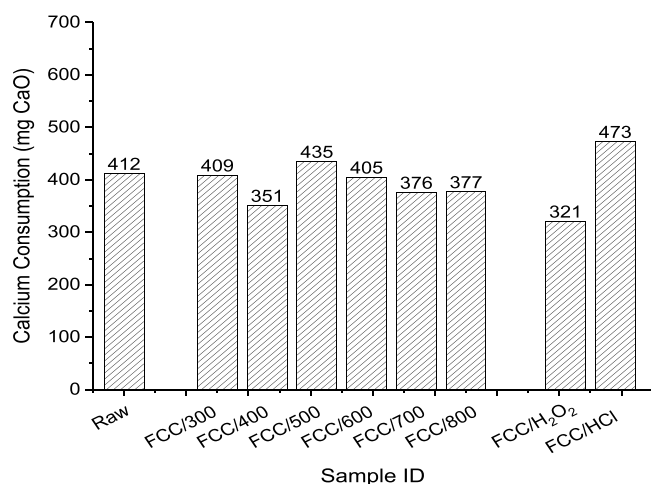**Fig. 8.** SEM micrograph of spent FCC particles calcined at 800 °C.

Fig. 9. Ca^{2+} consumption of the raw and treated spent FCC.

3.2. Reactivity by the Chapelle test

All the spent catalysts consume significant Ca^{2+} (Fig. 9) indicating a high early dissolution rate and high pozzolanic activity. The acid-etched catalyst displays the highest consumption, hence the strongest pozzolanic activity, while the oxidised catalyst has the lowest activity. The alkali-fused FCC was not tested as the unreacted CO_3^{2-} and/or OH^- produced during alkaline fusion would interfere with the results.

Calcination does not significantly impact the early activity of the catalyst (Fig. 9), but the highest temperatures (700–800 °C) slightly lowered Ca^{2+} consumption. The reduction of reactivity at high temperature is probably due to the partial collapse of the spent catalyst particles. The collapse is shown in the SEM images featuring smooth surfaces and disappearance of macropores (Fig. 8) which lower the specific surface area of the catalyst particles. Tseng et al. [72] state that spent FCC particles collapse when calcined, and that pore channels break, pores close and the SSA declines lowering reactivity.

Oxidation lowers early pozzolanic activity. This disagrees with Abubakar et al. [73] and Vaičiukynienė et al. [42] who regard oxidation as an efficient method for removing coke (deposited during catalytic cracking) and increase reactivity. The spent catalyst in this study contains little organic matter (only 1% wt loss between 105 and 950 °C-Table 4) hence oxidation did not show a significant beneficial effect on activity.

The results show that HCl-etching enhances early activity. Shi and Day [71] state that HCl etching can form a silica gel on the pozzolan surface that increases reactivity.

When compared with other pozzolanic materials tested with an identical method (Table 5), the spent FCC shows an early activity comparable to fly ash (FA), red mud (RM) and bauxite. Despite the coarse spheres comprising the spent FCC, the particles bind as much Ca^{2+} in pozzolanic reactions as highly reactive Al-based materials of layered structures such as RM and bauxite.

3.3. Water demand

Except for the carbonate fusion, the treatments hardly altered the rheology of the spent FCC pastes (Fig. 10). The paste made with Na_2CO_3-fused catalyst did not flow until the water content raised to w/b = 0.90, while the other pastes required less water to flow (w/b = 0.75). Carbonate fusion raised the water demand due to the presence of residual carbonates trona and natrite ($Na_3H(CO_3)_2$ and Na_2CO_3). Fusion with NaOH has a negligible impact on rheology due to a lack of residual carbonate. HCl-etching slightly enhances workability while oxidation doesn't affect it. Calcination does not significantly impact the rheology of the pastes. The SEM observations of smoother surfaces on the acid-etched and 800 °C calcined particles (Figs. 8 and 7b) are consistent with their higher flowability.

The spent FCC has a greater water demand than other pozzolanic/cementitious materials such as FA and GGBS (Fig. 10). At w/b = 0.60, the FA pastes reached a 165 mm initial flow diameter, but the catalyst pastes required more water (w/b = 0.75) to initially flow. The catalyst and FA particles are similarly regular and spherical. The higher water demand of the spent catalyst is due to the exceedingly porous nature of its faujasite particles. Porous surfaces of large specific surface areas are typical of catalysts [10,18]. The high early dissolution rate of the catalyst particles seen in the Chapelle test also contributes to the high-water demand. Despite its angular particles, GGBS has superior workability than the spent catalyst (Fig. 10). This is due to the dense, non-porous GGBS particles not absorbing any mixing water while the porous surfaces and open structure of the catalyst particles absorb water demanding more water to flow.

3.4. Setting time

The setting times of pastes made with raw and treated spent FCC were compared with FA pastes (Fig. 11). The catalyst and FA have comparable chemical composition, but the FA paste takes much longer to initially set than the catalyst paste (25 h vs 7–8 h). However, their final set is similar (32 vs 35 hrs -FCC vs FA).

The different early dissolution rate of FCC and FA is responsible for their divergent early set. The open structure and highly porous surface of the zeolite comprising the catalyst accelerates dissolution which speeds up the early set, whereas the FA shells take longer to dissolve in the lime solution. This agrees with Lei and Pavía [74] who state that dissolved Al^{3+} from FA was not detected in solution until 24 hours after the reaction.

The outstanding early activity of the spent FCC leading to a quick initial set is also due to its high active aluminium content: the SiO_2/Al_2O_3 of the catalyst is 0.85, while the FA has a much higher ratio at c. 2.58 [53]. It is well known that the SiO_2/Al_2O_3 ratio of pozzolans and cements determines the speed of their setting, because Al^{3+} dissolves faster than Si^{4+}, resulting in a higher concentration of ions at early ages which are available to form hydrates that speed up the setting of the pastes. However, once the shell broke, the FA and the FCC catalyst dissolved at a similar rate, resulting in comparable final setting times. The differing early set of the catalyst and the FA disagrees with their similar Ca^{2+} consumption in the Chapelle test. This may be due to slight measurement discrepancies, as the FA's Ca^{2+} consumption is from a different author.

Calcination does not significantly affect the initial set: the raw and calcined spent catalyst pastes achieve their initial set at c.9 hours, agreeing with their similar Ca^{2+} combination evidenced with the
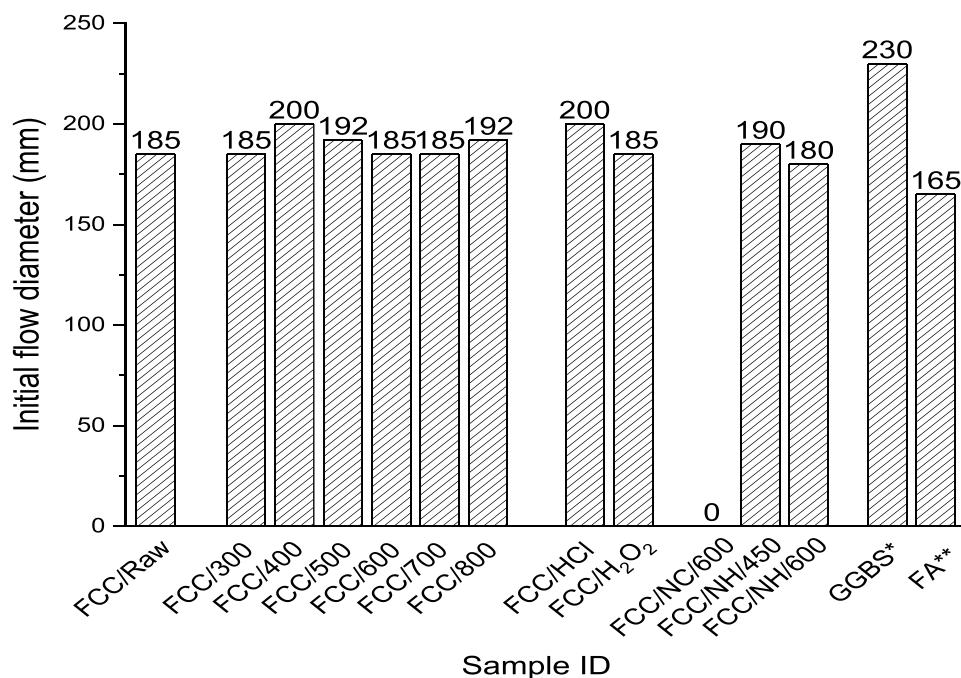
Fig. 10. Workability of spent FCC pastes compared with other pozzolanic and cementing materials, expressed as the initial flow diameter. W/b=0.75 except for FCC/NC/600 with w/b=0.90; *: w/b=0.75; **:w/b=0.60.
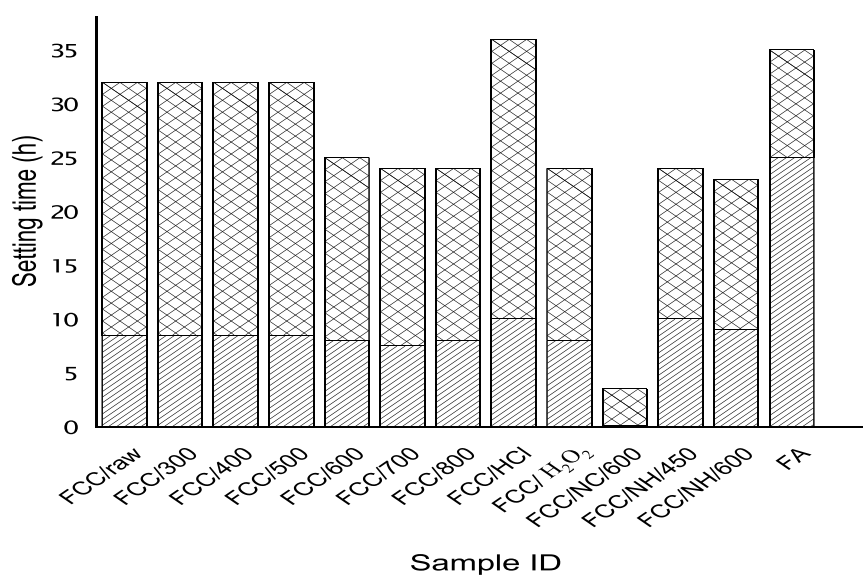

Fig. 11. Setting times of the spent FCC/lime pastes compared with FA.

Chapelle test. However, calcination above 500 °C shortens the final set (from 32 h to 24 h). A certain amorphization of the faujasite that increases reactivity may have taken place at the highest calcination temperatures. This was not evidenced with XRD however, partial particle/pore collapse was evidenced with SEM. Acid-etching delayed setting which may be due to the loss of ions during the treatment. Oxidation does not significantly affect setting, probably due to a lack of carbon, agreeing with the results above.

The paste prepared with Na$_2$CO$_3$-fused spent FCC (FCC/NC/800) sets extremely fast due to the quick reaction between Ca^{2+} from the lime and CO$_3^{2-}$ from the residual fusion carbonates, with an initial setting time of 5 mins and a final setting time of 3.5 h.

The NaOH-fused spent catalyst paste has an initial setting time like the raw catalyst and the calcined pastes (c.9 hours), but the final setting

time is shorter (24 h). The shortening of the final set is due to the amorphization of the faujasite during fusion (Fig. 6). A slightly faster set takes place when the NaOH fusion temperature increased to 600 °C which may be due to the presence of the hydraulic silicate N-A-S.

3.5. Reactivity by the mechanical activity index (MI)

In all cases, the MI is much greater than one, indicating high pozzolanic activity (Fig. 12). The MI results show that the spent catalyst has high reactivity, superior to pozzolans such as FA, red mud and RHA but lower than metakaolin (Table 6). The MI of the alkali-fused catalyst is comparable to GGBS.

The HCl-etched FCC has a slightly lower MI, possibly due to the loss of some active Al and Si through dissolution into the acid solution.
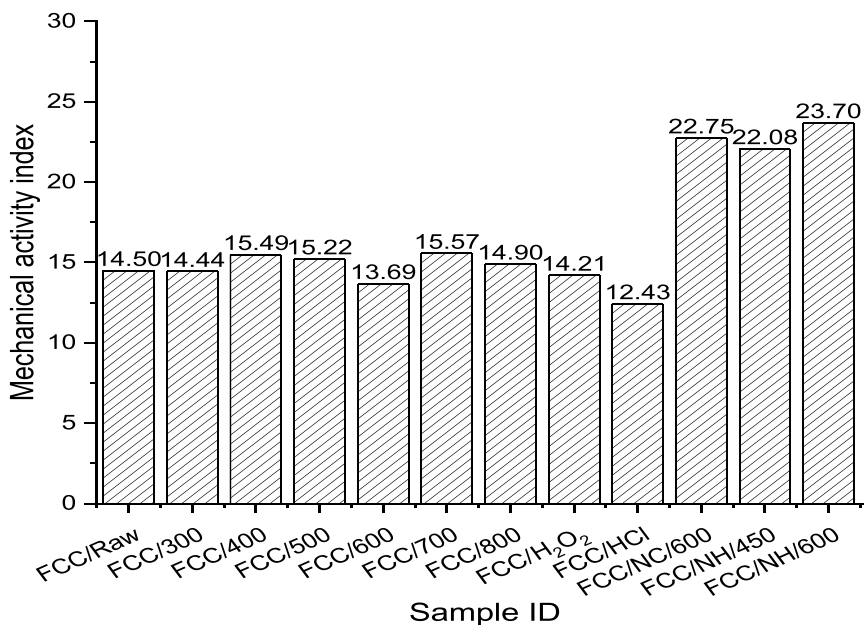
Fig. 12. Mechanical activity index of the spent FCC mortars (28 days).

Table 6
MI of the spent FCC compared with other pozzolanic and cementitious materials * [52] ** [75].

	FCC/Raw	FCC/NH/600	GGBS*	FA*	Metakaolin*	RHA*	Red Mud**
MI	14.5	23.7	29.5	3.4	38	12	6–8

Calcination does not significantly alter the MI which slightly fluctuates as the temperature increases agreeing with the Chapelle test and mineralogy results. Oxidation does not alter the MI as, due to the lack of carbon in the spent FCC, oxidation had a minor impact on the FCC's activity.

Alkali fusion enhanced the MI which achieved high values of 22–24. In particular NaOH-fusion at 600 °C (FCC/NH/600). This treatment

broke down the zeolite structure and generated a reactive amorphous phase and sodium aluminium silicate (N-A-S, Fig. 6) which are responsible for the high MI (24). NaOH-fusion at 450 °C (FCC/NH/450) which also broke and amorphized the faujasite (Fig. 6) provided a slightly lower MI (22). This suggests that the hydration of the N-A-S (only present at the highest fusion temperature) slightly contributes to strength up to 28 days. As seen in Section 3.8 (Composition of the cements), the high MI (23) of the carbonate-fused FCC (FCC/NC/600) is due to the presence of carbonates forming a calcite binder that increases density and strength.

3.7. Late strength development and mechanical behaviour

At 28 days, the raw, calcined and oxidised spent FCC specimens attain a compressive strength of ~6 MPa. Acid etching slightly lowers
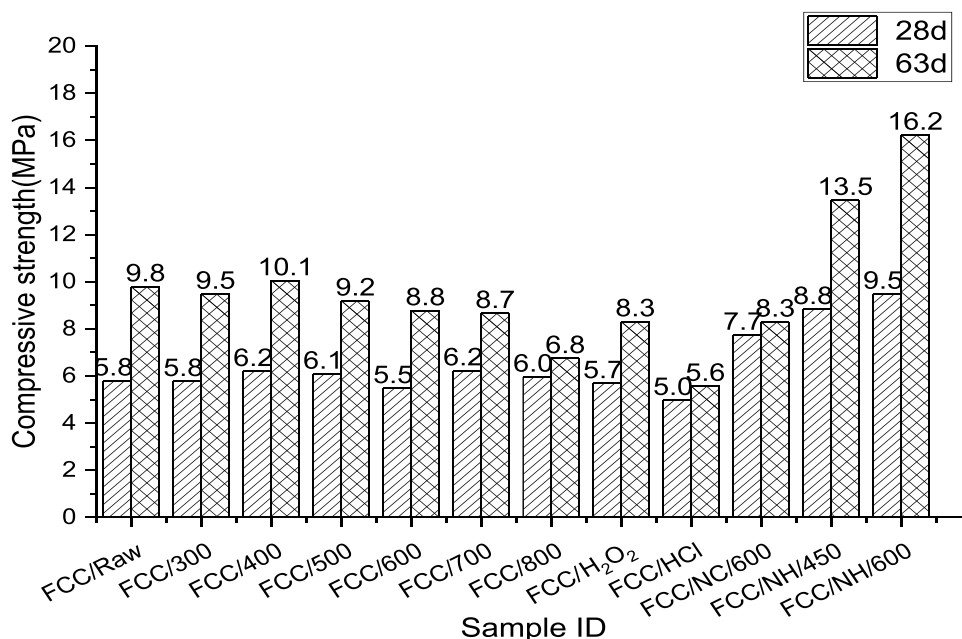

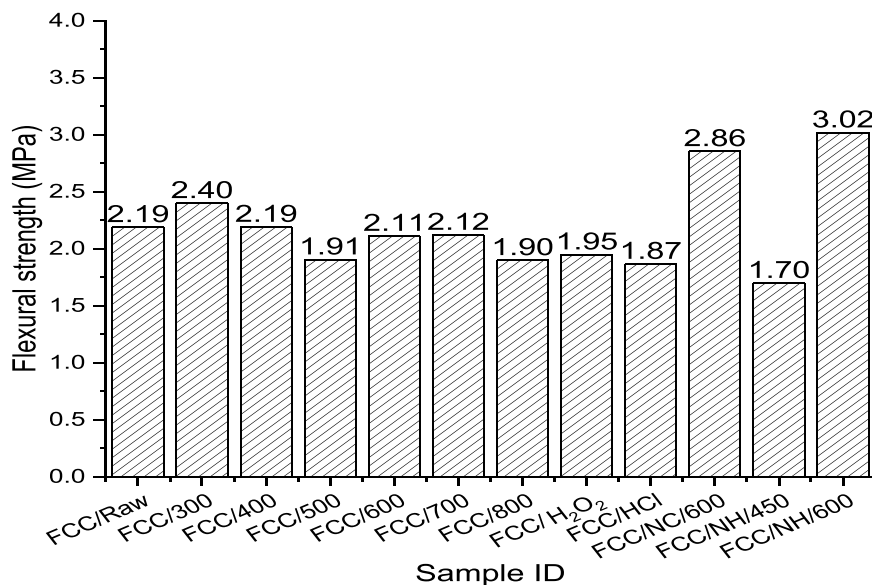**Fig. 13.** Compressive strength of spent FCC-lime mortars at 28 and 63 days.

Fig. 14. Flexural strength of spent FCC mortars at 28 days.

strength (5 MPa) while alkali-fusion increases it up to ~9.5 MPa (Fig. 13). In all cases, strength raises over time (28–63 days). The raw spent FCC specimens increased strength by 69% between 28 and 63 days. NaOH fusion at 600 °C led to the greatest late strength of over 16 MPa at 63 days.

The calcined spent FCC specimens increase strength considerably between 28 and 63 days except for the 800 °C specimens, with only 13% strength improvement, probably due to the partial collapse of the catalyst particles and their SSA reduction determined with the SEM. Increasing calcination temperature had no discernible effect on the 28-day strength, agreeing with the previous reactivity results. The thermal treatment did not significantly alter the mineral composition of the FCC (Figs. 4 and 5) therefore, the specimens reached similar strengths despite the difference in processing temperature.

The acid-etched and Na$_2$CO$_3$-fused specimens yield little strength improvement between 28 and 63 days, with 12 and 7.8% increase respectively. As discussed above, acid etching partially dissolves some soluble Si and Al from the FCC surface and form a gel. This might increase pozzolanic activity in the short-term, as demonstrated in the Chapelle test (~16 h), since gels react more readily with portlandite than zeolites. However, the loss of active Si and Al results in a strength reduction in the longer-term (specifically from 28 days onwards, as characterised in the MI and late strength results).

In Na$_2$CO$_3$ fusion, the carbonate residues react with Ca^{2+} forming a calcite cement that densifies the microstructure and yields a high compressive strength at 28d (7.7 MPa) but render a trivial improvement over time (8.3 MPa at 63 d). Furthermore, as seen above, carbonate fusion raises the water demand (w/b = 0.9 vs 0.75 for the other groups), a further reason for the low strength improvement over time.

NaOH-fusion amorphized the zeolite, plus it newforms a silicate at 600 °C (Fig. 6), these increase reactivity and enhance strength. NaOH fusion at 600 °C provides the highest late strength (16.2 MPa at 63d), increasing by over 70% between 28 and 63 days. This agrees with the former results, therefore the hydration of the silicate (N-A-S sintered during fusion) contributes to the 28d strength while the amorphous phase reacts more slowly raising the late strength to over 16 MPa at 63 days.

The flexural strength shows a similar trend to the compressive strength. The thermal treatment did not significantly impact the results. The raw, calcined, acid-etched and oxidised spent FCC specimens are within the c.1.90–2.40 MPa range. Fusion at 600 °C significantly improved flexural strength, especially the NaOH fusion. The strength

results agree with previous authors who report that the reaction between spent FCC and lime lasts for 90 days, whereby lime is progressively consumed to form carboaluminates, strätlingite and calcite which increase strength [76].

3.8. Composition of the cements in the FCC-lime pastes

In the raw and calcined spent FCC specimens, the XRD evidenced that the cements include monocarboaluminate- Ca$_4$Al$_2$O$_6$CO$_3$ 11H$_2$O – and minor calcite (Fig. 15) while the SEM/EDX shows semi-amorphous gels and plate C-A-H crystals in dense matrices (Figs. 16 and 17). The calcite cement is scarce because the Ca^{2+} from the lime has combined with aluminium to form carboaluminates. The silica in the zeolite has formed hydrates (C-S-H /C-A-S-H) which are clear from the SEM/EDX results but do not appear in the XRD analyses due to their low crystallinity and relative amount.

Monocarboaluminates belong to the group of AFm phases and are relatively common in Al-rich systems containing carbonate. According to Lothenbach et al. [77] and Moon et al. [78] monocarboaluminates have a high bulk modulus that can improve the strength of the cement matrix by lowering porosity.

In the carbonate-fused FCC, the XRD analyses indicate that calcite is the dominant cementing phase mixed with some carboaluminates. The excess CO$_3^{2-}$ has combined with the free Ca^{2+} to form calcite (Fig. 15). The SEM/EDX analyses show a cement of N-A-S-H gel mixed with abundant euhedral calcite (Fig. 18). The SEM also evidenced unreacted spent FCC (Fig. 18a). This agrees with the results above showing that the carbonate didn't react with the spent FCC during fusion because the fusion temperature was below the carbonate's melting point.

The significant difference in the nature of the cements in the raw/calcined and carbonate-fused FCC explains their difference in strength. The dominant calcite cement in the carbonate-fused FCC filled space quickly, improving the 28-day strength (Fig. 13) while, in the raw and the calcined FCC pastes, the C-S-H (or C-A-S-H) cements formed slowly due to the relatively slow dissolving rate of the zeolite contributing to the strength growth in the long term (Fig. 13).

The oxidised spent FCC paste (FCC/H$_2$O$_2$) includes fewer cementing hydrate gels and little densification (Fig. 19). In comparison with the calcined FCC (Fig. 17), the matrix of FCC/H$_2$O$_2$ is less dense and more porous, agreeing with the lower strength results.

In the NaOH-fused spent FCC paste, the XRD analyses evidenced cements of carboaluminate hydrates, calcite and portlandite (Fig. 15).
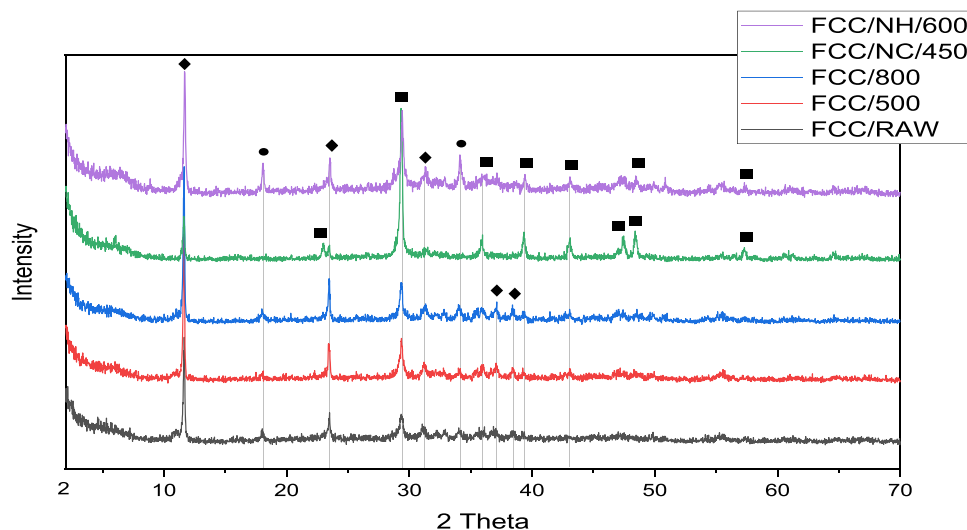
Fig. 15. Mineral composition of the cementing phases in the spent FCC-lime pastes at 28d ◆ Calcium Aluminium Oxide Carbonate Hydrate - $Ca_4Al_2O_6CO_3\,11H_2O$-. ■ Calcite - $CaCO_3$; ● Portlandite $Ca(OH)_2$.
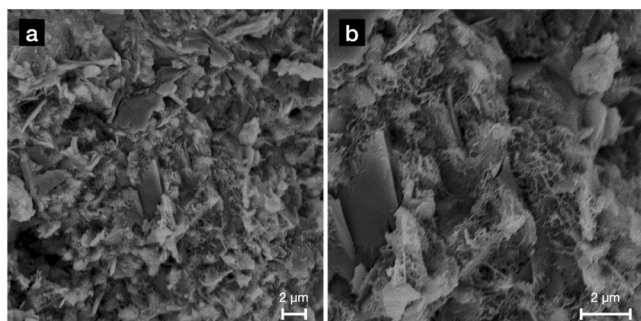

Fig. 16. Cementing phases in the pastes made with calcined spent FCC (FCC/400). (a) general (b) detail of hydrates with plate and gel structure.

The SEM analyses show hydrates covered with calcite crystals. According to the EDX results, the hydrates are C-A-S-H gels with high Ca/Si and Si/Al ratios (Figs. 20 and 21). They have a significantly higher Si/Al ratio than the cementing hydrates in the carbonate-fused FCC (Fig. 18) which is responsible for their higher strength (Fig. 13). This agrees with the results above, indicating that NaOH-fusion breaks down the zeolite

further than any other treatment, and dissolves Si which formed cementing hydrates of greater strength (Fig. 14).

4. Conclusion

The spent FCC waste is highly pozzolanic, even in raw form. It consists of faujasite, a reactive zeolite. The chemical composition results evidenced that SiO_2 and Al_2O_3 total over 90 wt%, and that heavy metals (present in either traces or minimal concentrations) can be immobilised in a matrix. Therefore, spent FCC waste can be used safely, as a pozzolan, in construction materials.

The raw FCC is considerably active, an efficient pozzolan with outstanding early activity (measured as Ca^{2+} consumption), and a fast early set (faster than FA) which delivers significant strength (6–10 MPa) and a high mechanical index (14).

Calcination alone (up to 800 °C) is not enough to cause the amorphization of the faujasite (and hence increase activity and enhance strength), but fusion with NaOH is highly efficient, even at low temperature (450 °C).

NaOH fusion breaks down the zeolite further than any other treatment. It dissolves Si^{4+} from the zeolite which forms cementing hydrates with high Ca/Si and Si/Al ratios that provide high strength. Fusing spent
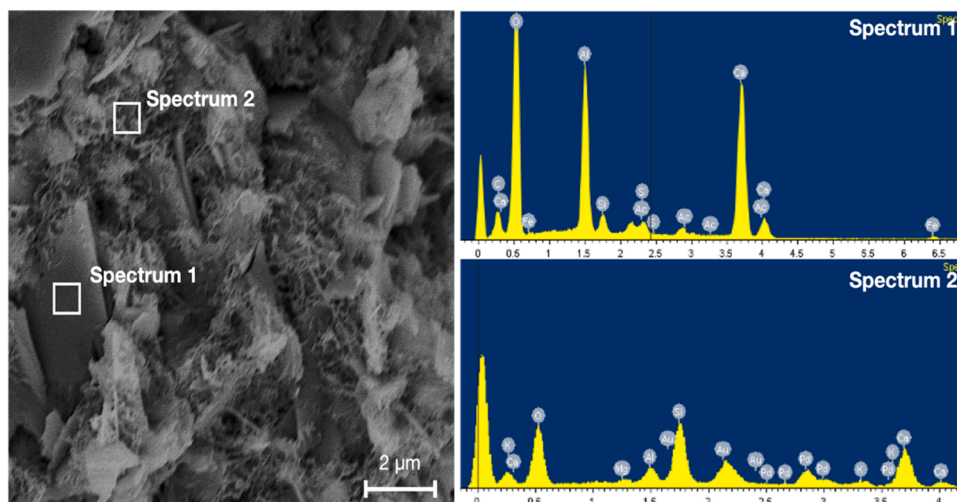

Fig. 17. Elemental composition of the cements in Fig. 16: hexagonal calcium carboaluminate hydrates (spectrum 1) and C-S-H cements (spectrum 2).
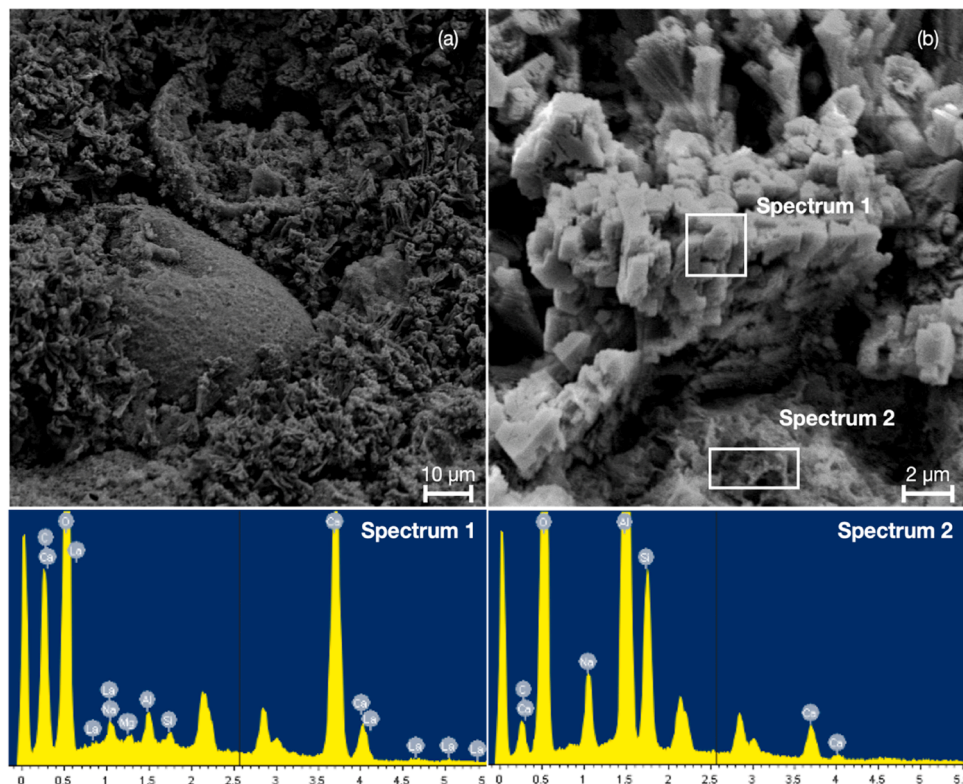
Fig. 18. Microstructure and composition of the pastes made with carbonate-fused FCC (a) general (b) detail of calcite (spectrum 1) and N-A-S-H cement (spectrum 2).
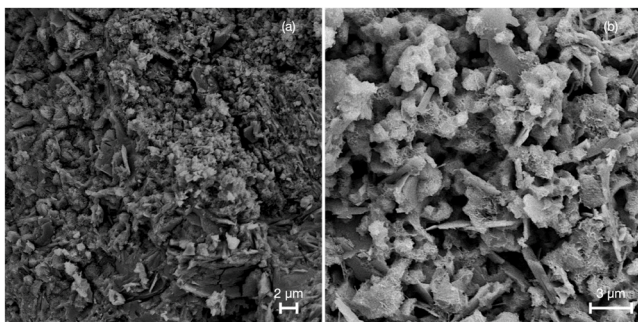

Fig. 19. Structure and cements in the pastes made with oxidised spent FCC (FCC/H_2O_2) (a) general (b) detail.

Fig. 20. Detail of the dense hydrates in the NaOH fused FCC specimens.

FCC, with NaOH, at 450 °C, transforms the zeolite into an amorphous phase which provides high strength (9–13 MPa at 28 and 63 days respectively) and a mechanical index of over 22, much superior to other pozzolans such as FA and RHA, closer to cementitious materials such as GGBS. Increasing the NaOH fusion temperature to 600 °C reorganises some of the amorphous phase into a hydraulic silicate (N-A-S) which forms cementing hydrates that provide the greatest strength (over 16 MPa at 63 days) and the highest mechanical index (24).

Acid etching improved activity in the short term (as demonstrated with the Chapelle test which runs for 16 hours). However, the acid partially dissolved the FCC particle surface with gel formation; and this removed some soluble Si/ Al which reduced the ultimate strength and prolonged the setting time. Therefore, initially, acid etching has a positive effect but in the long-term, it shows a negative effect.

Due to the low organic matter in spent FCC, the oxidation treatment did not increase reactivity.

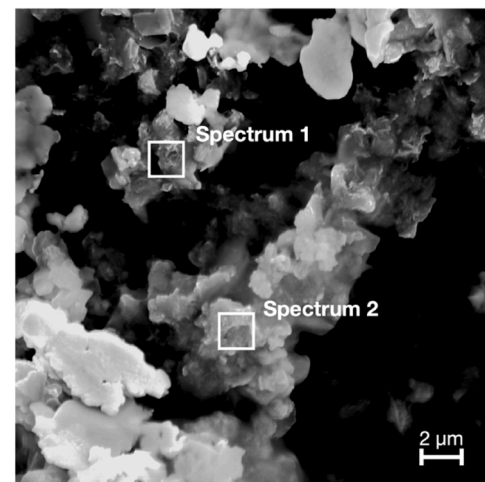Fusion with Na_2CO_3 needs a temperature above the melting point of the Na_2CO_3 to release significant alkalis and enhance reactivity and strength. A fusion temperature of 600 °C does not alter the spent FCC, but it only provides CO_3^{2-} that forms calcite cements which densify the matrix and provide early strength but lower long-term strength and workability.

Declaration of Competing Interest

The authors declare that they have no known competing financial interests or personal relationships that could have appeared to influence the work reported in this paper.
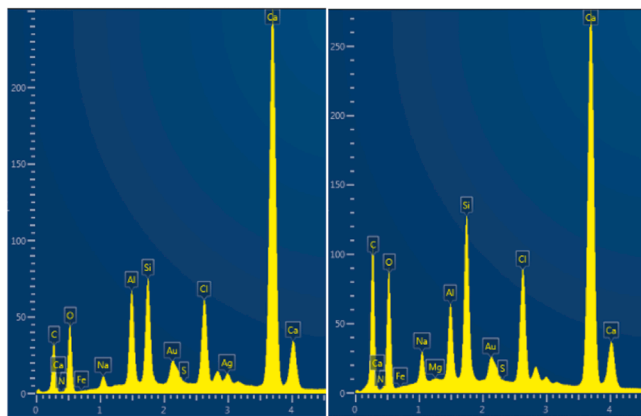
Fig. 21. Elemental composition of the hydrates by EDX.

Data availability

Data will be made available on request.

References

[1] Wojciechowski B.W., & Corma A. (1986). Catalytic Cracking: Catalysts, Chemistry, and Kinetics. https://www.osti.gov/biblio/6509096.

[2] M. Marafi, A. Stanislaus, Spent catalyst waste management: a review: part I—developments in hydroprocessing catalyst waste reduction and use, Resour. Conserv. Recycl. 52 (6) (2008) 859–873, https://doi.org/10.1016/j.resconrec.2008.02.004.

[3] M.R. Gonzalez, A.M. Pereyra, P. Bosch, G. Fetter, V.H. Lara, E.I. Basaldella, Structural and morphological evolutions of spent FCC catalyst pellets toward NaA zeolite, J. Mater. Sci. 51 (11) (2016) 5061–5072, https://doi.org/10.1007/s10853-016-9809-7.

[4] A. Akcil, F. Vegliò, F. Ferella, M.D. Okudan, A. Tuncuk, A review of metal recovery from spent petroleum catalysts and ash, Waste Manag. 45 (2015) 420–433, https://doi.org/10.1016/j.wasman.2015.07.007 (Oxford).

[5] H. Cheng, K.L. Lin, R. Cui, C.L. Hwang, Y.M. Chang, T.W. Cheng, The effects of SiO2/Na2O molar ratio on the characteristics of alkali-activated waste catalyst–metakaolin based geopolymers, Constr. Build. Mater. 95 (2015) 710–720, https://doi.org/10.1016/j.conbuildmat.2015.07.028.

[6] H.S. Cerqueira, G. Caeiro, L. Costa, F. Ramôa Ribeiro, Deactivation of FCC catalysts, J. Mol. Catal. A Chem. 292 (1) (2008) 1–13, https://doi.org/10.1016/j.molcata.2008.06.014.

[7] T. Chiranjeevi, R. Pragya, S. Gupta, D.T. Gokak, S. Bhargava, Minimization of waste spent catalyst in refineries, Procedia Environ. Sci. 35 (2016) 610–617, https://doi.org/10.1016/j.proenv.2016.07.047.

[8] H. Fu, Y. Chen, T. Liu, X. Zhu, Y. Yang, H. Song, Research on hazardous waste removal management: identification of the hazardous characteristics of fluid catalytic cracking spent catalysts, Molecules 26 (2021) 2289, https://doi.org/10.3390/molecules26082289.

[9] Y.J. Wang, C. Wang, L.L. Li, Y. Chen, C.H. He, L. Zheng, Assessment of ecotoxicity of spent fluid catalytic cracking (FCC) refinery catalysts on Raphidocelis subcapitata and predictive models for toxicity, Ecotoxicol. Environ. Saf. 222 (2021), 112466.

[10] H.L. Chen, Y.S. Tseng, K.C. Hsu, Spent FCC catalyst as a pozzolanic material for high-performance mortars, Cem. Concr. Compos. 26 (6) (2004) 657–664, https://doi.org/10.1016/S0958-9465(03)00048-9.

[11] EPA, Reference document for hazardous waste listings. Hazardous Substances (Classification) Notice 2017, U.S. Environmental Protection Agency, 2017. https://www.epa.gov/hw/userfriendly-refence-document-hazardous-waste-listings.

[12] United States Environmental Protection Agency (USEPA), Hazardous waste management system, Fed. Regist. 68 (202) (2003) 59935–59940.

[13] EU Commission Decision, Amending decision 2000/532/EC on the list of waste pursuant to directive 2008/98/EC, OJ L 370 (2014) 44–86.

[14] Ministry of Ecology and Environment of the People's Republic of China (MEERC, National Hazardous Waste List, Ministry of Ecology and Environment of the People's Republic of China, 2021.

[15] D. Sun, X.Z. Li, M. Brungs, D. Trimm, Encapsulation of Heavy Metals On Spent Fluid Catalytic Cracking Catalyst, 38, Water Science and Technology, 1998, pp. 211–217, https://doi.org/10.1016/S0273-1223(98)00530-7. IssuesISSN 0273-1223.

[16] P. Duxson, J.L. Provis, G.C. Lukey, J.S.J. van Deventer, The role of inorganic polymer technology in the development of 'green concrete, Cem. Concr. Res. 37 (12) (2007) 1590–1597, https://doi.org/10.1016/j.cemconres.2007.08.018.

[17] O. Alelweet, S. Pavia, Pozzolanic and hydraulic activity of bauxite for binder production, J. Build. Eng. 51 (2022), 104186, https://doi.org/10.1016/j.jobe.2022.104186.

[18] J. Rouquerol, P. Llewellyn, K. Sing, Adsorption by clays, pillared layer structures and zeolites. Adsorption by Powders and Porous Solids, 2013, pp. 467–527, https://doi.org/10.1016/B978-0-08-097035-6.00012-7.

[19] R. Sadeghbeigi, Chapter 5—FCC catalysts. Fluid Catalytic Cracking Handbook, 4th Ed., Butterworth-Heinemann, 2020, pp. 83–110, https://doi.org/10.1016/B978-0-12-812663-9.00005-9.

[20] B. Liguori, P. Aprea, B.d. Gennaro, F. Iucolano, A. Colella, D. Caputo, Pozzolanic Activity of Zeolites The Role of Si/Al Ratio, Materials 12 (2019) 4231, https://doi.org/10.3390/ma12244231.

[21] B. Pacewska, I. Wilińska, J. Kubissa, Use of spent catalyst from catalytic cracking in fluidized bed as a new concrete additive, Thermochim. Acta 322 (2) (1998) 175–181.

[22] J. Payá, J. Monzó, M.V. Borrachero, Fluid catalytic cracking catalyst residue (FC3R): an excellent mineral by-product for improving early-strength development of cement mixtures, Cem. Concr. Res. 29 (11) (1999) 1773–1779.

[23] J. Payá, J. Monzó, M.V. Borrachero, S. Velázquez, Evaluation of the pozzolanic activity of fluid catalytic cracking catalyst residue (FC3R). Thermogravimetric analysis studies on FC3R-Portland cement pastes, Cem. Concr. Res. 33 (4) (2003) 603–609, https://doi.org/10.1016/S0008-8846(02)01026-8.

[24] N. Su, H.Y. Fang, Z.H. Chen, F.S. Liu, Reuse of waste catalysts from petrochemical industries for cement substitution, Cem. Concr. Res. 30 (11) (2000) 1773–1783.

[25] J. Payá, J. Monzó, M.V. Borrachero, Physical, chemical and mechanical properties of fluid catalytic cracking catalyst residue (FC3R) blended cements, Cem. Concr. Res. 31 (1) (2001) 57–61.

[26] J.H. Wu, W.L. Wu, K.C. Hsu, The effect of waste oil-cracking catalyst on the compressive strength of cement pastes and mortars, Cem. Concr. Res. 33 (2) (2003) 245–253.

[27] J. Dweck, C.A. Pinto, P.M. Büchler, Study of a Brazilian spent catalyst as cement aggregate by thermal and mechanical analysis, J. Therm. Anal. Calorim. 92 (2008) 121–127.

[28] R.C. Mielenz, L.P. Witte, O.J. Glantz, Effect of calcination on natural pozzolans, in: Proceedings of the Symposium on Use of Pozzolanic Materials in Mortars and Concretes, 1950.

[29] S. Ferreiro, M.M.C. Canut, J. Lund, D. Herfort, Influence of fineness of raw clay and calcination temperature on the performance of calcined clay-limestone blended cements, Appl. Clay Sci. 169 (2019) 81–90, https://doi.org/10.1016/j.clay.2018.12.021.

[30] A. Tironi, M.A. Trezza, A.N. Scian, E.F. Irassar, Assessment of pozzolanic activity of different calcined clays, Cem. Concr. Compos. 37 (2013) 319–327, https://doi.org/10.1016/j.cemconcomp.2013.01.002.

[31] R. García, R. Vigil de la Villa, M. Frías, O. Rodriguez, S. Martínez-Ramírez, L. Fernández-Carrasco, I.S. de Soto, E Villar-Cociña, Mineralogical study of calcined coal waste in a pozzolan/Ca(OH)2 system, Appl. Clay Sci. 108 (2015) 45–54, https://doi.org/10.1016/j.clay.2015.02.014.

[32] R. Vigil de la Villa, M. Frías, R. García-Giménez, S. Martínez-Ramirez, L Fernández-Carrasco, Chemical and mineral transformations that occur in mine waste and washery rejects during pre-utilization calcination, Int. J. Coal Geol. 132 (2014) 123–130, https://doi.org/10.1016/j.coal.2014.07.014.

[33] R. García, R.V. de la Villa, I. Vegas, M. Frías, M.S. de Rojas, The pozzolanic properties of paper sludge waste, Constr. Build. Mater. 22 (7) (2008) 1484–1490.

[34] M. Frias, E. Villar-Cocina, E. Valencia-Morales, Characterisation of sugar cane straw waste as pozzolanic material for construction: calcining temperature and kinetic parameters, Waste Manag. 27 (4) (2007) 533–538 (Oxford).

[35] F Bergaya, T.G. Lagaly, Handbook of Clay Science, Elsevier, 2006.

[36] R.L. Figueiredo, S. Pavía, A study of the parameters that determine the reactivity of sugarcane bagasse ashes (SCBA) for use as a binder in construction, SN Appl. Sci. 2 (2020) 1–15.

[37] Z. Lei, S. Pavia, Reactivity of raw, pyroprocessed and GGBS-blended alum sludge (AS) waste for sustainable cement production, J. Build. Eng. 65 (2023), 105787, https://doi.org/10.1016/j.jobe.2022.105787.

[38] S. Pavía, R. Walker, P. Veale, A. Wood, Impact of the properties and reactivity of rice husk ash on lime mortar properties, J. Mater. Civ. Eng. 26 (9) (2014), 04014066.

[39] O. Alelweet, S. Pavia, A comparative study of the environmental impact of alkali activated and traditional materials, Civil Eng. Res. (2022) 613–618. Ireland. Holmes, De Paor, WestISBN 978-0-9573957-5-6. Publ. by Civil Eng. Research Association of Ireland.

[40] A.H. Ismail, A. Kusbiantoro, S.C. Chin, K. Muthusamy, M. Islam, K.F. Tee, Pozzolanic reactivity and strength activity index of mortar containing palm oil

clinker pretreated with hydrochloric acid, J. Cleaner Prod. 242 (2020), 118565, https://doi.org/10.1016/j.jclepro.2019.118565.

[41] C.P.F. de Lima, G.C. Cordeiro, Evaluation of corn straw ash as supplementary cementitious material: Effect of acid leaching on its pozzolanic activity, Cement 4 (2021), 100007, https://doi.org/10.1016/j.cement.2021.100007.

[42] D. Vaičiukynienė, A. Grinys, V. Vaitkevičius, A. Kantautas, Purified waste FCC catalyst as a cement replacement material, Ceram. Silik. 59 (2) (2015) 103–108.

[43] L. Ayele, J. Pérez-Pariente, Y. Chebude, I. Díaz, Conventional versus alkali fusion synthesis of zeolite A from low grade kaolin, Appl. Clay Sci. 132–133 (2016) 485–490, https://doi.org/10.1016/j.clay.2016.07.019.

[44] X. Guo, J. Liu, H. Qin, Y. Liu, Q. Tian, D. Li, Recovery of metal values from waste printed circuit boards using an alkali fusion–leaching–separation process, Hydrometallurgy 156 (2015) 199–205, https://doi.org/10.1016/j.hydromet.2015.06.011.

[45] D. Li, X. Guo, Z. Xu, Q. Tian, Q. Feng, Leaching behavior of metals from copper anode slime using an alkali fusion-leaching process, Hydrometallurgy 157 (2015) 9–12, https://doi.org/10.1016/j.hydromet.2015.07.008.

[46] H. Ma, Q. Yao, Y. Fu, C. Ma, X. Dong, Synthesis of zeolite of type A from bentonite by alkali fusion activation using Na_2CO_3, Ind. Eng. Chem. Res. 49 (2) (2010) 454–458, https://doi.org/10.1021/ie901205y.

[47] T. Wajima, Y. Ikegami, Synthesis of crystalline zeolite-13X from waste porcelain using alkali fusion, Ceram. Int. 35 (7) (2009) 2983–2986, https://doi.org/10.1016/j.ceramint.2009.03.014.

[48] Q. Mao, Y. Li, K. Liu, H. Peng, X. Shi, Mechanism, characterization and factors of reaction between basalt and alkali: exploratory investigation for potential application in geopolymer concrete, Cem. Concr. Compos. 130 (2022), 104526, https://doi.org/10.1016/j.cemconcomp.2022.104526.

[49] Q. Liu, M. Cui, X. Li, J. Wang, Z. Wang, L. Li, X. Lyu, Alkali-hydrothermal activation of mine tailings to prepare one-part geopolymer: Activation mechanism, workability, strength, and hydration reaction, Ceram. Int. 48 (20) (2022) 30407–30417, https://doi.org/10.1016/j.ceramint.2022.06.318.

[50] EN 1015-3: 2007 Methods of test for mortar for masonry-part, 3.

[51] T. Liu, Z. Qiu, J. Yang, X. Mei, L. Cao, W. Zhang, Morphological, composition analysis, and environmental risks assessment of spent FCC catalysts, Inorg. Chem. Ind. 48 (11) (2016) 71–74.

[52] R. Walker, S. Pavía, Physical properties and reactivity of pozzolans, and their influence on the properties of lime–pozzolan pastes, Mater. Struct. 44 (6) (2011) 1139–1150, https://doi.org/10.1617/s11527-010-9689-2.

[53] O. Alelweet, S. Pavia, K. Ruane, V. Jaksic, Potential of a low-calcium fly ash (FA) for the production of alkali-activated materials, in: Proceedings of the Civil Engineering Research Ireland (CERI) Conf, Publ. by Civil Eng. Res. Association of Ireland, 2020, pp. 162–167.

[54] S. Pavia, O. Alelweet, Durability of alkali-activated materials made with a high-calcium, basic slag, Recent Prog. Mater. 3 (4) (2021) 1. –1.

[55] P.B. Tchounwou, C.G. Yedjou, A.K. Patlolla, D.J. Sutton, A. Luch, Heavy metal toxicity and the environment. Molecular, Clinical Andenvironmental Toxicology: Volume 3: Environmental Toxicology, Springer, 2012, pp. 133–164, https://doi.org/10.1007/978-3-7643-8340-4_6.

[56] RAIS, Toxicity Profiles Formal Toxicity Summary for VANADIUM U.S, Department of Energy (DOE) and the University of Tennessee, 2020. https://rais.ornl.gov/tox/profiles/vanadium_f_V1.html.

[57] C. Buttice, Nickel compounds. Colditz GA. The SAGE Encyclopedia of Cancer and Society, Second Edition, SAGE Publications, Inc, 2015, pp. 828–831.

[58] J. Emsley, Nature's Building Blocks: An A-Z Guide to the Elements, Oxford University Press, 2011, pp. 266–277. ISBN 9780199605637.

[59] A. Dufresne, G. Krier, J. Muller, B. Case, G. Perrault, Lanthanide particles in the lung of a printer, Sci. Total Environ. 151 (3) (1994) 249–252, https://doi.org/10.1016/0048-9697(94)90474-X.

[60] P.M. Waring, R.J. Watling, Rare earth deposits in a deceased movie projectionist. a new case of rare earth pneumoconiosis, Med. J. Aust. 153 (11–12) (1990) 726–730, https://doi.org/10.5694/j.1326-5377.1990.tb126334.

[61] C.E.T. Vogt, M.B. Weckhuysen, Fluid catalytic cracking: recent developments on the grand old lady of zeolite catalysis, Chem. Soc. Rev. 44 (20) (2015) 7342–7370, https://doi.org/10.1039/C5CS00376H.

[62] M.P. Gómez-Tena, J. Gilabert, J. Toledo, E. Zumaquero, C. Machí, Relationship between the specific surface area parameters determined using different analytical techniques, in: Proceedings of the XII Foro Global Del Recubrimiento Cerámico, Universitat Jaume I, Castellón, Spain, 2014, pp. 17–18.

[63] B. Pacewska, M. Bukowska, I. Wilińska, M. Swat, Modification of the properties of concrete by a new pozzolan—a waste catalyst from the catalytic process in a fluidized bed, Cem. Concr. Res. 32 (1) (2002) 145–152, https://doi.org/10.1016/S0008-8846(01)00646-9.

[64] I.M. Kolesnikov, I.N. Frolova, Production and activity of sillimanite and sillmanite-zeolite aluminosilicate catalysts, J. Appl. Chem. 55 (3) (1982). USSR (Engl. Transl.); (United States), https://www.osti.gov/biblio/6287940.

[65] E.D. Rodríguez, S.A. Bernal, J.L. Provis, J.D. Gehman, J.M. Monzó, J. Payá, M. V. Borrachero, Geopolymers based on spent catalyst residue from a fluid catalytic cracking (FCC) process, Fuel 109 (2013) 493–502, https://doi.org/10.1016/j.fuel.2013.02.053.

[66] Hernández-Beltrán F., Mogica-Martínez E., López-Salinas E., & Elena Llanos-Serrano M. (2000). TPR and CO2-TPD of composite titania (anatase)-alumina systems as potential vanadium traps for fluid catalytic cracking (FCC). In A. Corma, F.V. Melo, S. Mendioroz, & J. Fierro, L. G. (Eds.), Studies in Surface Science and Catalysis (Vol. 130, pp. 2459–2464). Elsevier. 10.1016/S0167-2991(00)80838-1.

[67] C.Y. Li, L.V. Rees, The thermal stability of faujasites with different SiAl ratios, Zeolites 6 (1) (1986) 60–65.

[68] A.E. Newkirk, I. Aliferis, Drying and decomposition of sodium carbonate, Anal. Chem. 30 (5) (1958) 982–984.

[69] D. Feng, J.L. Provis, J.S.J. van Deventer, Thermal activation of albite for the synthesis of one-part mix geopolymers, J. Am. Ceram. Soc. 95 (2) (2012) 565–572, https://doi.org/10.1111/j.1551-2916.2011.04925.x.

[70] I.H. Choi, G. Moon, J.Y. Lee, R.K. Jyothi, Alkali fusion using sodium carbonate for extraction of vanadium and tungsten for the preparation of synthetic sodium titanate from spent SCR catalyst, Sci. Rep. 9 (1) (2019), https://doi.org/10.1038/s41598-019-48767-0. Article 1.

[71] C. Shi, R.L. Day, Comparison of different methods for enhancing reactivity of pozzolans, Cem. Concr. Res. 31 (5) (2001) 813–818, https://doi.org/10.1016/S0008-8846(01)00481-1.

[72] Y.S. Tseng, C.L. Huang, K.C. Hsu, The pozzolanic activity of a calcined waste FCC catalyst and its effect on the compressive strength of cementitious materials, Cem. Concr. Res. 35 (4) (2005) 782–787, https://doi.org/10.1016/j.cemconres.2004.04.026.

[73] A. Abubakar, I.E. Waba, S. Yunusa, N. Audu, Reactivation of spent FCC catalyst via oxidation and acid treatment, Appl. J. Environ. Eng. Sci. 6 (1) (2020) 22–34, 6-1 (2020).

[74] Z. Lei, S. Pavía, Effect of the early dissolution of Al-phases in reactive industrial wastes, on the setting times and rheology of sustainable binders, Civil Eng. Res. 1 (2022) 34–38.

[75] O. Alelweet, S. Pavia, Z. Lei, Pozzolanic and cementing activity of raw and pyro-processed saudi arabian red mud (RM) waste, Recent Prog. Mater. 3 (4) (2021), 4, https://doi.org/10.21926/rpm.2104047. Article.

[76] A.R. Villca, L. Soriano, A. Font, M.M. Tashima, J. Monzó, M. Victoria Borrachero, J. Payá, Lime/pozzolan/geopolymer systems: performance in pastes and mortars, Constr. Build. Mater. 276 (2021), 122208, https://doi.org/10.1016/j.conbuildmat.2020.122208.

[77] B. Lothenbach, G. Le Saout, E. Gallucci, K. Scrivener, Influence of limestone on the hydration of Portland cements, Cem. Concr. Res. 38 (6) (2008) 848–860.

[78] J. Moon, J.E. Oh, M. Balonis, F.P. Glasser, S.M. Clark, P.J. Monteiro, High pressure study of low compressibility tetracalcium aluminum carbonate hydrates 3CaO· Al_2O_3· $CaCO_3$· $11H_2O$, Cem. Concr. Res. 42 (1) (2012) 105–110.